Simulation of Lattice Dendrimers by a Monte Carlo Technique with Detailed Balance

Marc L. Mansfield*

Department of Chemistry and Chemical Biology, Stevens Institute of Technology, Hoboken, New Jersey 07030

Miyoun Jeong

Department of Chemical, Biochemical and Materials Engineering, Stevens Institute of Technology, Hoboken, New Jersey 07030

Received December 26, 2001; Revised Manuscript Received June 26, 2002

ABSTRACT: We have published extensively on a lattice dendrimer model whose properties were simulated by a Monte Carlo technique. However, it has recently been pointed out that the simulation technique violated detailed balance and that the ensuing errors, at least for dendrimers without excluded volume, were relatively large. In this contribution we show how the technique can be efficiently modified to satisfy detailed balance, and we report results on dendrimers as high as $G = 11$. When applied to dendrimers with excluded volume, we find that the older technique generates only relatively small errors, and we are therefore confident that our previous results are qualitatively valid. We also discuss our model in light of recent neutron scattering studies concerned with the distribution of end groups.

Introduction

We have developed a technique for studying lattice dendrimers by Monte Carlo simulation.[1−4] A significant advantage of this technique over other approaches is the ability to simulate high generation dendrimers. For example, we are currently able to obtain useful data on $G = 11$ dendrimers, while atomic-resolution molecular dynamics calculations currently only reach about 4 or 5 generations.[5−10] However, Wallace, Buzza, and Read[11] recently pointed out that our Monte Carlo procedure fails to satisfy detailed balance. The procedure performs "wiggles" on the lattice dendrimer and relies on the accumulation of a large number of random wiggles to generate ensemble averages of lattice dendrimers with excluded volume. Failure to satisfy detailed balance, of course, introduces a bias and skews the ensemble away from equilibrium.

The wiggles are of two types, end wiggles and internal wiggles (Figure 1), and detailed balance problems occur only with the internal wiggles. The internal wiggle involves the three spacers connected at a common branch point. Tentative new positions for the branch point were selected at random from one of the 12 points $\mathbf{r} = (\pm2,\pm2,0)$, $\mathbf{r} = (\pm2,0,\pm2)$, $\mathbf{r} = (0,\pm2,\pm2)$, where $\mathbf{r}$ is the current position of the branch point, and it is this selection technique that leads to the problem.[11] One way to avoid the problem is to select a new configuration for the three spacers from among all possibilities. The total number of such configurations can often be very large, and so the problem of selecting an arbitrary one does seem to be prohibitively expensive. However, the approach described in the following section provides an efficient technique that properly weights each tentative configuration.

Technique

The new technique differs from the old one[1−4] only in the execution of internal wiggles, and so here we describe only those modifications. Individual states of each spacer are all possible seven-step walks on the lattice for which the reverse of any one step is forbidden. The first step can occur in any one of four directions on the lattice, while suppression of the back step means that all subsequent steps can occur in only three ways. Therefore, there are $4\cdot3^6 = 2916$ possible states for each spacer. For each site on the lattice, we define the "accessible set" to be the set of all lattice points that are the end points of these seven-step walks, and if $\mathbf{x}$ is in the accessible set of $\mathbf{x_0}$, then we let $n(\mathbf{x} - \mathbf{x_0})$ represent the total number of unique seven-step walks that leave $\mathbf{x_0}$ and arrive at $\mathbf{x}$. We have, by explicit enumeration, tabulated the values of $n(\mathbf{x} - \mathbf{x_0})$ for all possible values of $\mathbf{x} - \mathbf{x_0}$ and find that the accessible set of any point contains 216 points in all.

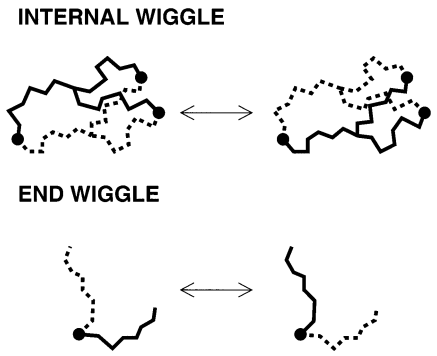

Figure 1. Ensembles of dendrimer structures are generated by a technique that relies on the accumulation of large numbers of wiggles. There are two kinds of wiggles, internal and end wiggles.

Once a set of three spacers has been chosen to be wiggled, we erase the three spacers (Figure 2) and generate a new tentative conformation for them. To satisfy detailed balance, the new conformation must be chosen without bias from among the full set of possible conformations. The selection process is summarized in Figure 2. Designate the three end points as $\mathbf{x_a}$, $\mathbf{x_b}$, and $\mathbf{x_c}$. Each of these possesses its own accessible set, **A**, **B**,

10.1021/ma012229k CCC: $22.00
Published on Web 11/01/2002

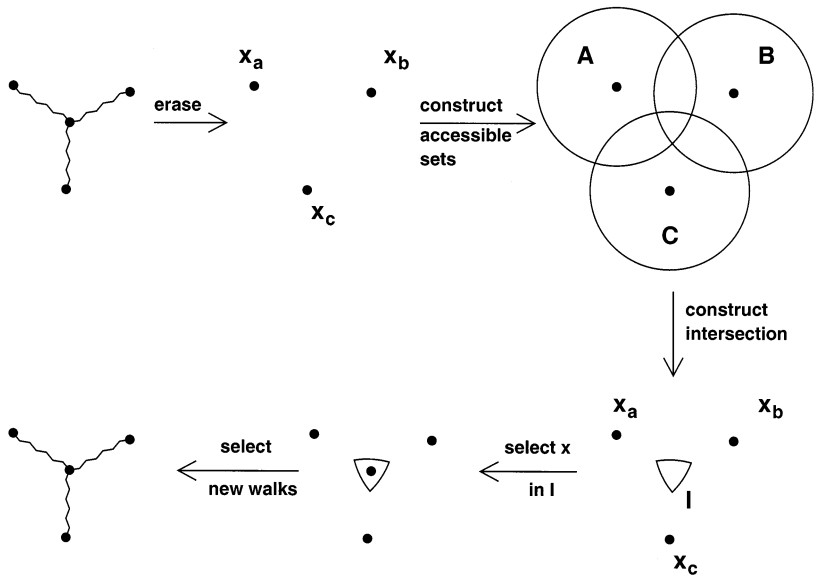

Figure 2. An internal wiggle begins with the selection of three spacers meeting at a common branch point. The common branch point and the three spacers are erased from the structure, leaving the three branch points $\mathbf{x_a}$, $\mathbf{x_b}$, and $\mathbf{x_c}$. The "accessible set" **A**, defined as the set of all lattice sites accessible from $\mathbf{x_a}$ in seven steps, is then constructed, followed by the constructions of **B** and **C**, which are the accessible sets of $\mathbf{x_b}$ and $\mathbf{x_c}$, respectively. The set **I**, representing the intersection of **A**, **B**, and **C**, is then constructed. (**I** is never empty; we know it always contains at least the original branch point.) A new branch point is selected from **I**, and then new spacers are selected. The text describes how this selection is done so that the choice is unbiased.

and **C**, respectively. Then we construct **I** as the intersection of **A**, **B**, and **C**. Obviously, the new position of the node must be selected from **I**, but each point $\mathbf{x} \in \mathbf{I}$ must be weighted with $n(\mathbf{x} - \mathbf{x_a})\, n(\mathbf{x} - \mathbf{x_b})\, n(\mathbf{x} - \mathbf{x_c})$, the total number of possible conformations of the three spacers, when one end of each is at $\mathbf{x_a}$, $\mathbf{x_b}$, and $\mathbf{x_c}$, respectively, and when the other end is at **x**. Therefore, we calculate

$$N = \sum_{\mathbf{x} \in \mathbf{I}} n(\mathbf{x} - \mathbf{x_a})\, n(\mathbf{x} - \mathbf{x_b})\, n(\mathbf{x} - \mathbf{x_c}) \qquad (1)$$

and select at random an integer J in the interval $[0, N - 1]$. Then, for each point $\mathbf{x} \in \mathbf{I}$ we begin subtracting $n(\mathbf{x} - \mathbf{x_a})\, n(\mathbf{x} - \mathbf{x_b})\, n(\mathbf{x} - \mathbf{x_c})$ from J and stop when the difference first falls below zero. The value of **x** at which this happens is taken as the new tentative position of the node, and J is redefined to take on its last positive value. Then we take $k_a = \mathrm{mod}\,(J, n(\mathbf{x} - \mathbf{x_a}))$, $J' = \{(J - k_a)\}/\{n(\mathbf{x} - \mathbf{x_a})\}$, $k_b = \mathrm{mod}\,(J', n(\mathbf{x} - \mathbf{x_b}))$, and $k_c = \{(J' - k_b)\}/\{n(\mathbf{x} - \mathbf{x_b})\}$ and, finally, redefine k_a, k_b, and k_c to be $k_a + 1$, $k_b + 1$, and $k_c + 1$, respectively. Then of the $n(\mathbf{x} - \mathbf{x_a})$ walks extending from $\mathbf{x_a}$ to **x**, we select the k_a-th one, and similar selections provide the walks extending from $\mathbf{x_b}$ to **x** and $\mathbf{x_c}$ to **x**. This new conformation is accepted unconditionally if we are not enforcing excluded volume constraints, but if we are it is only accepted if it does not increase the number of pairwise overlaps. Otherwise, the previous conformation is restored. Whether the new conformation is accepted or not, the wiggle count advances by one, since, by the rules of Metropolis Monte Carlo, a restored conformation must be permitted to contribute again to the ensemble.

The most efficient method of forming the intersection **I** of the three sets **A**, **B**, and **C** is to impose a sorting order on all lattice points: (x,y,z) appears before (x',y',z') if $x < x'$; while if $x = x'$, then the y values determine the sorting order, unless these are also equal, and then of course the order is determined by the z values. We can easily design our procedure so that all three sets **A**, **B**, and **C** are automatically generated in this sorting order. Then we simultaneously examine the entries at the top of all three lists. If they are all equal, we record this entry on the list for **I** and remove it from the lists for **A**, **B**, and **C**. If the top three entries are not all equal, we remove the one(s) that occur first in sorting order. This continues until at least one of the three lists is exhausted.

Wallace et al.[11] demonstrated the impropriety of the original technique by computing the radius of gyration without excluded volume, since this can be done independently by a different method. We have done the same and find that the method outlined above agrees to within sampling error with an approach in which the dendrimers are grown directly.

Comparisons between the Two Approaches

Wallace et al.[11] reported significant differences between the predictions of the two approaches when applied to models without excluded volume, but they performed no comparisons when excluded-volume constraints are included. Their results cast doubt on the results of our previous work,[1−4] since rather significant discrepancies are observed. However, as we now show, the differences between the two procedures are relatively modest under excluded-volume conditions.

Each internal wiggle now takes longer to execute, but relaxation occurs much more rapidly. Table 1 compares estimates of relaxation times, given in units of "megawiggles," defined as the time required for the gyration radius of artificially expanded or compressed structures to stabilize. On Pentium III machines we are able to do about one megawiggle of simulation in a minute of CPU time and are able to obtain useful results on models as high as generation 11. Figure 3 displays R_g, R_h, and the intrinsic viscosity and compares them with the analogous values computed without detailed balance. These quantities are also summarized in Table 2. (See refs 4 and 12−21 for a description of the technique for

Table 1. Relaxation Statistics[a]

G	relaxation time (Mwiggles)	sampling interval (Mwiggles)
1	≪1	0.25
2	<1	0.5
3	<1	0.75
4	<1	1
5	1	1
6	2	2
7	8	8
8	30	30
9	50	50
10	100	100
11	200	200

[a] The relaxation time is the number of Monte Carlo steps, in units of 10^6 wiggles, required for the gyration radius of artificially perturbed dendrimers to relax. The sampling interval is the number of wiggles between samples of the system and is intended to be large enough that subsequent samples are at least largely statistically independent.

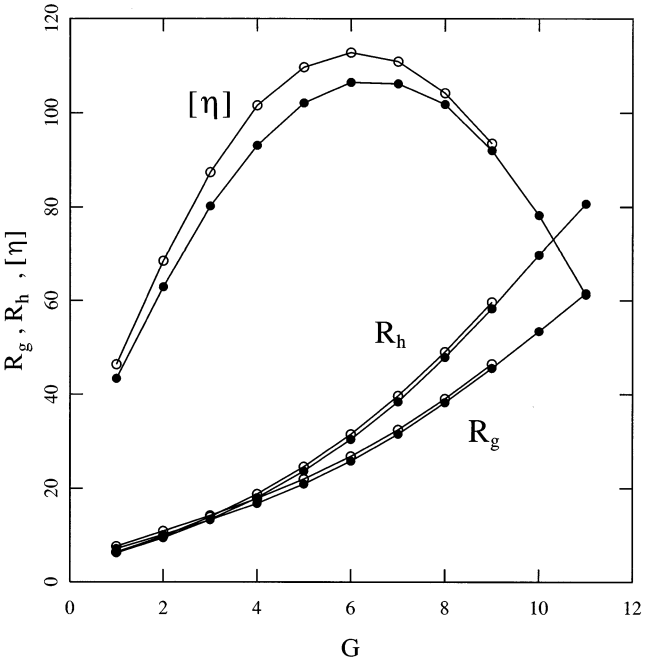

Figure 3. Comparison between gyration radii (R_g), hydrodynamic radii (R_h), and intrinsic viscosity ([η]) as calculated either by the older technique (open circles) or by the newer one (filled circles). Length and mass units are such that the nearest-neighbor distance on the lattice is $3^{1/2}$ and that the mass of a dendrimer equals the number of occupied lattice sites.

calculating the hydrodynamic properties.) The radial density profiles are also in reasonably good agreement. Figure 4 shows these for $G = 8$ as computed by both simulation procedures. Similar agreement is obtained at all generations. Furthermore, the model continues to display a broad distribution of end groups, with end groups distributed throughout the molecule, as displayed for $G = 8$ in Figure 5. Figures 4 and 5 display the "volume fraction" as a function of distance from the core, which for this model is defined as the fraction of lattice sites in spherical shells that are occupied by segments of the dendrimer. In summary, the rather large differences observed by Wallace et al.[11] on "phantom" dendrimers, without excluded volume, become much smaller when we examine dendrimers with excluded volume. Our previous results[1–4] are incorrect, but the discrepancies are not as serious as we have been led to believe by the calculations on phantom dendrimers.

Table 2. Results of Simulations[a]

G	$R_{g,int}$	R_g	$R_{g,end}$	R_h	[η]
1	4.38	7.13	8.07	6.21	43.4
2	7.53	10.10	11.59	9.43	62.9
3	10.80	13.28	15.08	13.34	80.2
4	14.41	16.79	18.73	17.99	93.1
5	18.67	20.93	22.90	23.69	102.1
6	23.71	25.82	27.74	30.45	106.5
7	29.57	31.56	33.40	38.42	106.2
8	36.38	38.24	40.01	47.88	101.8
9	43.72	45.56	47.33	58.28	92.0
10	51.50	53.42	55.28	69.74	78.2
11	59.35	61.51	63.60	80.66	61.2

[a] Length and mass units are such that the nearest neighbor distance on the lattice is $3^{1/2}$, and the mass of a dendrimer is equal to the number of lattice sites it occupies.

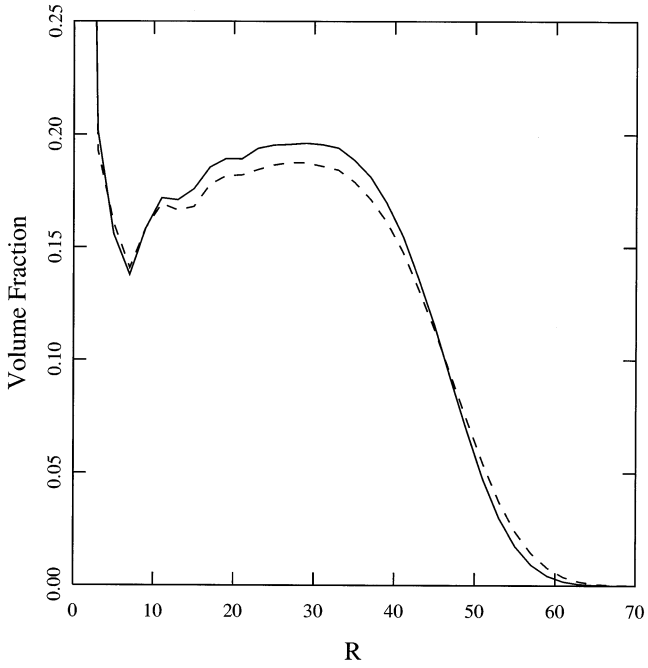

Figure 4. Radial density (measured as the fraction of occupied lattice sites) of the $G = 8$ dendrimer, calculated either by the older technique (dashed curve) or by the newer one (solid curve).

End Group Distribution

Topp et al.[22] have performed neutron scattering experiments on poly(amido amine) dendrimers in which only the terminal units are deuterated. These experiments yield the gyration radius of only the terminal groups of the dendrimer, $R_{g,end}$. The value of $R_{g,end}$ relative to R_g illuminates the controversial question of the distribution of terminal groups in the dendrimer. To provide a comparison with these experiments, we have calculated $R_{g,end}$ for the current model as well as the radius of gyration assuming that all segments but those in the terminal generation are labeled, $R_{g,int}$. All three gyration radii are given in Table 2. As expected, $R_{g,int} < R_g < R_{g,end}$. Figure 6 displays the results of these calculations as a fractional difference in R_g, i.e., as either $(R_{g,end} - R_g)/R_g$ or $(R_{g,int} - R_g)/R_g$. Figure 6 also shows the experimental value of Topp et al.[22] for $G = 7$ PAMAM dendrimers, $(R_{g,end} - R_g)/R_g = 0.14 \pm 0.036$, and an estimate of Lyulin et al.[9] obtained by Brownian dynamics simulation of a $G = 5$ bead model dendrimer,

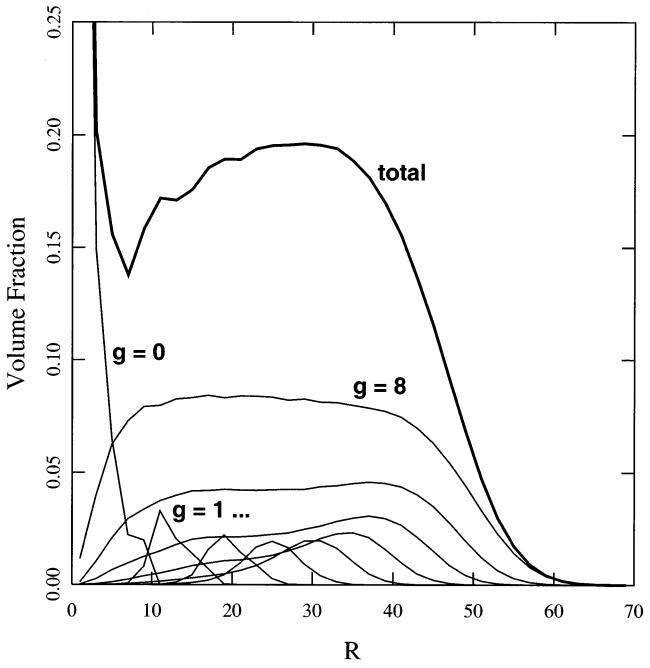

Figure 5. Radial density (measured as the fraction of occupied lattice sites) of the $G = 8$ dendrimer, calculated by the newer technique, showing contributions from each tier of the dendrimer.

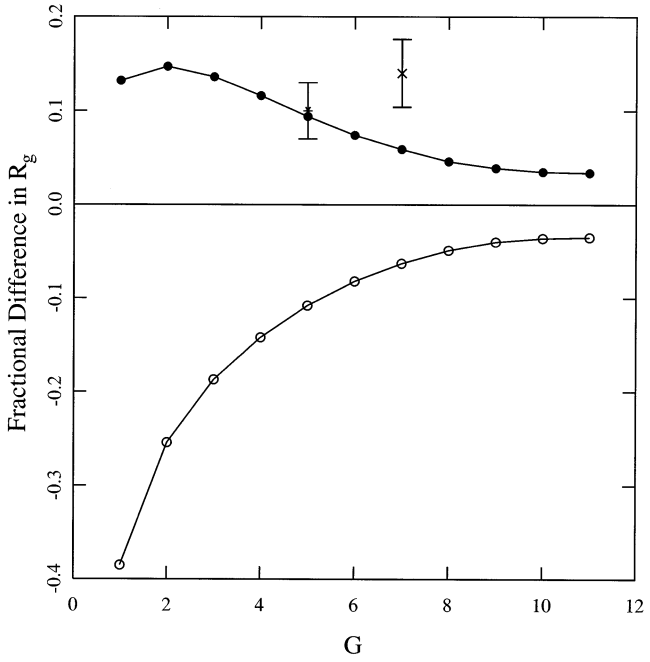

Figure 6. Relative difference in R_g between: model dendrimers in which internal segments are labeled (open circles); model dendrimers in which end segments are labeled (filled circles); the experimental results of Topp et al.[22] (cross with error bars); and the model dendrimers of Lyulin et al.[9] (asterisk with error bars).

$(R_{g,end} - R_g)/R_g = 0.10 \pm 0.03$. The Lyulin et al. result agrees well with our result at the same G value, but if comparisons are to be made only at the same value of G, our model is unable to predict the Topp et al. result. Furthermore, experience with simple models[23,24] seems to imply that if $(R_{g,end} - R_g)/R_g$ is as large as 0.14, then the distribution of the terminal groups must be quite different from that of the complete molecule; i.e., segregation of the end groups to the periphery is more significant in the PAMAM dendrimers than it is in this model. By contrast, there is experimental NMR evidence for end groups in close proximity to the core of poly(benzyl ether) dendrimers over a range of generations.[25,26] Furthermore, neutron scattering results[27,28] for the radial density distribution of $G = 4$ and $G = 5$ dendrimers have been interpreted to indicate a density maximum at the core, although data for dendrimers in which only the ends are labeled are not available, and as we have already pointed out,[4] the particle scattering factors for our model are in good qualitative agreement with the experimental SAXS data[29] for PAMAM dendrimers. Given these conflicting results, the best conclusion seems to be that the distribution of the ends is nonuniversal, perhaps resembling this model in some cases but with stronger segregation in others.

Summary

We have demonstrated an efficient technique that avoids the detailed balance pitfall of our previous dendrimer calculations. According to Wallace, Buzza, and Read,[11] the failure to satisfy detailed balance leads to significant discrepancies in the properties of "phantom" dendrimers, but we find that the discrepancies are relatively small when the dendrimers have excluded volume. The radius of gyration, the hydrodynamic radius, the intrinsic viscosity, and the radial density function computed by either method agree rather well. Given these results, we are confident that all the qualitative findings of our previous publications[1−4] still hold. Furthermore, the new technique is about as efficient as the old one; each Monte Carlo step does take longer, but the algorithm explores phase space more efficiently.

Our model is unable to satisfactorily explain the neutron scattering data of Topp et al..,[22] who measured the radius of gyration of PAMAM dendrimers when only the end groups are labeled. Their results seem to indicate that the end groups of the PAMAM dendrimers are more strongly segregated to the exterior of the molecule than they are in this model.

Acknowledgment. We thank Prof. D. M. A. Buzza for kindly providing a manuscript[30] prior to publication.

Note Added in Proof. A similar solution to the same problem has been developed by Giupponi and Buzza (*Macromolecules* **2002**, *35*, 9799).

Note Added after ASAP Posting

This article was released ASAP on 11/01/2002 without the Note Added in Proof and reference 30. The correct version was posted on 11/22/2002.

References and Notes

(1) Mansfield, M. L.; Klushin, L. I. *Macromolecules* **1993**, *26*, 4262.
(2) Mansfield, M. L. *Polymer* **1994**, *35*, 1827.
(3) Mansfield, M. L. *Polymer* **1996**, *37*, 3835.
(4) Mansfield, M. L. *Macromolecules* **2000**, *33*, 8043.
(5) Sournies, F.; Crasnier, F.; Vidal, C.; Labarre, M.-C.; Labarre, J.-F. *Main Group Chem.* **1996**, *1*, 207.
(6) Murat, M.; Grest, G. S. *Macromolecules* **1996**, *26*, 1278.
(7) Miklis, P.; Çagin, T.; Goddard, W. A., III *J. Am. Chem. Soc.* **1997**, *119*, 7458.
(8) Lach, C.; Brizzolara, D.; Frey, H. *Macromol. Theory Simul.* **1997**, *6*, 371.
(9) Lyulin, A. V.; Davies, G. R.; Adolf, D. B. *Macromolecules* **2000**, *33*, 6899.
(10) Gorman, C. B.; Smith, J. C. *Polymer* **2000**, *41*, 675.

(11) Wallace, E. J.; Buzza, D. M. A.; Read, D. J. *Macromolecules* **2001**, *34*, 7140.
(12) Luty, B. A.; McCammon, J. A.; Zhou, H.-X. *J. Chem. Phys.* **1992**, *97*, 5682.
(13) Hubbard, J. B.; Douglas, J. F. *Phys. Rev. E* **1993**, *47*, 2986.
(14) Douglas, J. F.; Zhou, H.-X.; Hubbard, J. B. *Phys. Rev. E* **1994**, *49*, 5319.
(15) Zhou, H.-X.; Szabo, A.; Douglas, J. F.; Hubbard, J. B. *J. Chem. Phys.* **1994**, *100*, 3821.
(16) Douglas, J. F.; Garboczi, E. J. *Adv. Chem. Phys.* **1995**, *91*, 85.
(17) Douglas, J. F.; Friedman, A. Coping with Complex Boundaries. In *IMA Series on Mathematics and its Applications*; Springer: New York, 1995; Vol. 67, p 166.
(18) Garboczi, E. J.; Douglas, J. F. *Phys. Rev. E* **1996**, *53*, 6169.
(19) Given, J. A.; Hubbard, J. B.; Douglas, J. F. *J. Chem. Phys.* **1997**, *106*, 3761.
(20) Douglas, J. F. *Adv. Chem. Phys.* **1997**, *102*, 121.
(21) Mansfield, M. L.; Douglas, J. F.; Garboczi, E. J. *Phys. Rev. E* **2001**, *64*, 61401.
(22) Topp, A.; Bauer, B. J.; Klimash, J. W.; Spindler, R.; Tomalia, D. A.; Amis, E. J. *Macromolecules* **1999**, *32*, 7226.
(23) Douglas, J. F., private communication.
(24) Mansfield, M. L., unpublished results.
(25) Wooley, K. L.; Klug, C. A.; Tasaki, K.; Schaefer, J. *J. Am. Chem. Soc.* **1997**, *119*, 53.
(26) Gorman, C. B.; Hager, M. W.; Parkhurst, B. L.; Smith, J. C. *Macromolecules* **1998**, *31*, 815.
(27) Pötschke, D.; Ballauff, M.; Lindner, P.; Fischer, M.; Vögtle, F. *Macromolecules* **1999**, *32*, 4079.
(28) Pötschke, D.; Ballauff, M.; Lindner, P.; Fischer, M.; Vögtle, F. *Macromol. Chem. Phys.* **2000**, *201*, 330.
(29) Bauer, B. J.; Topp, A.; Prosa, T. J.; Amis, E. J.; Yin, R.; Qin, D.; Tomalia, D. A. *Proc. ACS Div. Polym. Mater. Sci. Eng.* **1997**, *77*, 87.
(30) Giupponi, G.; Buzza, D. M. A. *Macromolecules* **2002**, *35*, 9799.

MA012229K